*29th EPS Conference on Plasma Phys. and Contr. Fusion Montreux, 17-21 June 2002 ECA Vol. **26B**, P-2.105 (2002)*

Effects of the Tilt of Magnetic Field Lines on Electron Acceleration in Front of LH Grills and on Ensuing Plasma Flows, Density Perturbations and Charge Separation Fields

V. Petrzilka, V. Fuchs, R. Klima, L. Krlin, P. Pavlo, R. Panek and F. Zacek
Association Euratom/IPP.CR, Prague, Czech Republic
M. Goniche, J. Gunn and Y. Peysson
Association Euratom/CEA Cadarache, France

Summary: We performed a 3-d two-fluid analysis of perturbations arising because of generation of fast electrons by LH waves in a thin layer just in front of the grill mouth. We found that rather significant plasma density perturbations, electrostatic charge separation fields and plasma flows (plasma vortex) can develop just in front of the grill mouth as a consequence of the electron acceleration and of the ensuing Coulomb separation potential. Our model does not predict significant variations of the vortex intensity with the B-tilt.

Basic equations and assumptions

We present a 3-d two-fluid analysis of the plasma vortex, which arises because of local generation of fast electrons by LH waves in a thin layer just in front of the grill mouth [1]: As the electrons are pushed away from the grill mouth along the magnetostatic field lines, they leave the heavier ions behind, and thus an electrostatic field and consequent plasma flows are generated. For the modeling, we developed an advanced version of our numerical code [2]. The code now does not require additional assumptions of a rather fast toroidal rotation. By using test particle simulations of electron acceleration for parameters relevant to conditions of the Tore Supra LH grill, it is possible to determine an effective potential W, which expels and accelerates the electron fluid [3]. We assume that, in front of one waveguide row, W is of the following form, $W = AM(c_s)^2\ [1 + \cos(2\pi z/L_g)] \sin(\pi y/L_{pol}) \exp(-x/L_{rf})$, where L_g and L_{pol} denote the toroidal and poloidal dimensions of the grill waveguide row, and L_{rf} denote the radial scale length of the electron acceleration decrease into the plasma interior. For the unperturbed plasma density and temperature, we choose step and ramp profiles, $n = n_0\ (1+x/\lambda_n)$, $T_{e,i} = T_{e,i0}(1 + x/L_T)$. For computations, the following set of momentum and continuity equations is used:

$$0 = -neE_x - \frac{\partial p_e}{\partial x} - \frac{ne}{c} v_y B_z \tag{1}$$

$$0 = -neE_y - \frac{\partial p_e}{\partial y} + \frac{ne}{c} v_x B_z \tag{2}$$

$$0 = -neE_z - \frac{\partial W}{\partial z} - \frac{\partial p_e}{\partial z} \tag{3}$$

$$Mn\frac{\partial V_x}{\partial t} + Mn(V_x\frac{\partial}{\partial x} + V_y\frac{\partial}{\partial y} + V_z\frac{\partial}{\partial z})V_x = neE_x - \frac{\partial p_i}{\partial x} + \frac{ne}{c}V_y B_z - MV_x S \tag{4}$$

$$Mn\frac{\partial V_y}{\partial t} + Mn(V_x\frac{\partial}{\partial x} + V_y\frac{\partial}{\partial y} + V_z\frac{\partial}{\partial z})V_y = neE_y - \frac{\partial p_i}{\partial y} - \frac{ne}{c}V_x B_z - MV_y S \tag{5}$$

$$Mn\frac{\partial V_z}{\partial t} + Mn(V_x\frac{\partial}{\partial x} + V_y\frac{\partial}{\partial y} + V_z\frac{\partial}{\partial z})V_z = neE_z - \frac{\partial p_i}{\partial z} - MV_z S \tag{6}$$

$$\frac{\partial n}{\partial t}+\frac{\partial}{\partial x}(nV_x)+\frac{\partial}{\partial y}(nV_y)+\frac{\partial}{\partial z}(nV_z)=S \qquad (7)$$

In the above equations, M denotes the ion mass, S denotes the source, **v** and **V** denote the electron and ion velocity, respectively. The other notation is standard. For the source term S, we assume that $S = D_\perp n/(\lambda_n)^2 + S_i = C\, D_\perp n/(\lambda_n)^2$, where the term S_i and/or the value of C represent ionization. In Eqs. (1-3), the electron inertia is neglected. The numerical algorithm proceeds as follows: In computations, the new density value is computed from (7). Then, E_z is computed from Eq. (3), and its value is then used in Eq. (6) in computations of new values of V_z . From the values of E_z on the x,y,z mesh, also the electrostatic potential U is computed by integration, and then the values of E_x and E_y are computed from U. Finally, the new values of V_x and V_y are determined from Eqs. (4) and (5).

Results of computations

In its current version, we are able to run the code for rather a short time of up to several microseconds only. Because of the relatively short time of computations, the final equilibrium state is not reached, and the solutions with various values of sources do not differ qualitatively. Therefore, we just choose the case with zero sources for the presentation. Typical results of the computations are shown in following Figures, for A = 8 (i.e., the maximum of W equals 400 eV, what corresponds to acceleration for the rf field of about 3 kV/cm at the waveguide mouth), for C = 0 (i.e. zero sources) and for other parameters close to the Tore Supra parameters: $n_0 = 2\text{x}10^{18}\text{cm}^{-3}$, $T_{e,i0} = 25$ eV, $D_\perp = 1$ m^2/s at the boundary, $\lambda_n = 1$ cm, $L_T = 3$ cm, $L_g = 30$ cm, $L_{pol} = 10$ cm, $L_{rf} = 2$ cm.

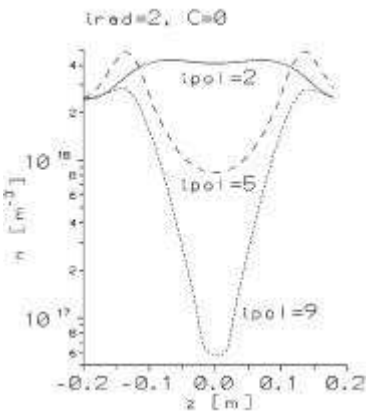

Fig. 1. Plasma density profile.

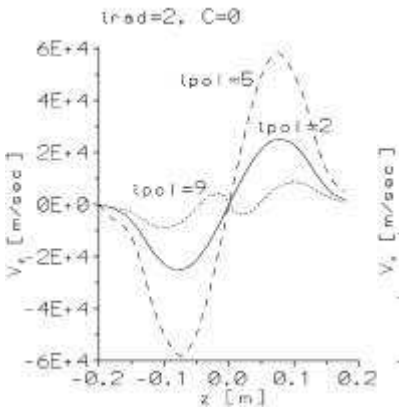

Fig. 2. Profile of the toroidal plasma flow velocity.

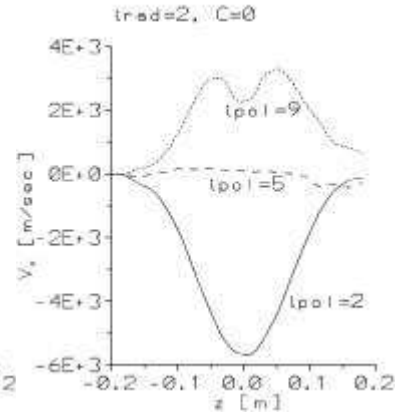

Fig. 3. Profile of the radial plasma flow velocity.

The results presented in the figures show the toroidal z-profiles for several values of the x (irad = 1,…,9) and y (ipol = 1,…,9) mesh. The value irad = 1 corresponds to x = 0 just at the grill mouth, while irad = 9 corresponds to the radial distance of x = 2 cm from the grill mouth. The value irad = 2, which is shown in the figures, then corresponds to x = 0.25 cm. Similarly, ipol = 1 corresponds to the value of the poloidal coordinate y = 0 at the grill row boundary (poloidally), the value ipol = 9 corresponds to the other poloidal boundary of the row (to y = 10 cm in our model computations). The value ipol = 5 then corresponds to y = 5 cm, poloidally in the middle of the waveguide row. In positions radially more distant from the grill mouth, i.e., for values of irad larger than 2, the profiles of all computed quantities are similar to those in the Figures, but their variation

as related to their unperturbed values is smaller. The value of the driving force, which is proportional to the value of W, decreases very quickly into the plasma interior.

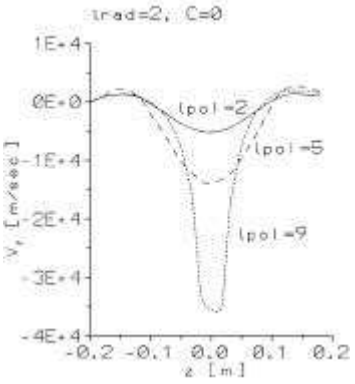

Fig. 4. Profile of the poloidal plasma flow velocity.

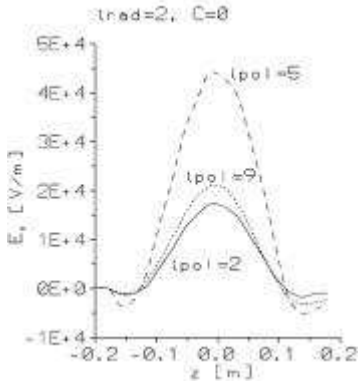

Fig. 5. Profile of the radial electrostatic field intensity.

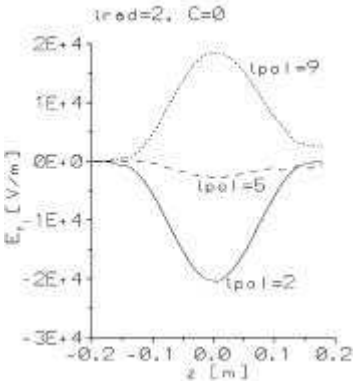

Fig. 6. Profile of the poloidal electrostatic field intensity.

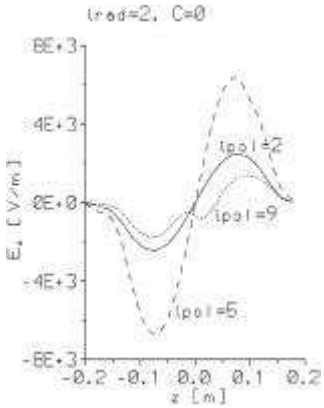

Fig. 7. Profile of the toroidal electrostatic field intensity.

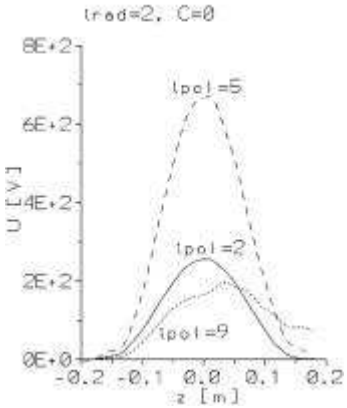

Fig. 8. Profile of the electrostatic potential.

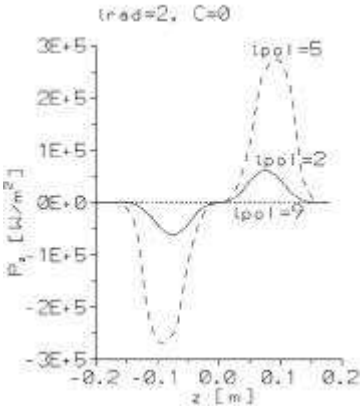

Fig. 9. Profile of the toroidal power density flow carried by the ion fluid.

We now estimate, using the above described model of one waveguide row, the vortex variations at magnetic tilt changes. When the plasma current changes, the poloidal magnetostatic field changes, too, and therefore also the angle between the magnetostatic field and the toroidal direction and the safety factor q vary at the plasma boundary in front of the grill mouth. The grill is oriented along the toroidal direction, and therefore the number of waveguides along various magnetic field lines varies. Some magnetic field lines intersect the row just at its corners, and there the length of the electron trajectory L_{eff} along the magnetic field is the shortest one. Now, let us present estimates of the variations of the L_{eff} shortening averaged for all possible electron trajectories, arising because of the tilt of the magnetic field lines. For a simple discussion of the spectra variations arising because of L_{eff} variations, let us consider a rectangle with the width equal to the half of the poloidal width of waveguides, and with the length equal to the grill length L_0, on the surface of which the Poynting vector S is maximum (S is approximately of the poloidal form of $\sin^2$). In Figure 10, the profiles of L_{eff}/L_0 are computed for values of q varying between 1 and 10, for geometrical parameters relevant to "old" and "new" Tore Supra launchers. We can see that, for realistic values of q between 3 and 9 at the plasma boundary, the values of L_{eff} / L_0 and

delta $N_{//}$ / delta $N_{//0}$ significantly vary by up to about 30%. As only one waveguide row was considered, the above estimates probably can exaggerate the L_{eff} and spectra width variations, as they do not take into account continuations of B-lines on other waveguide rows. Therefore, we also calculated the $N_{//}$ spectrum in the real geometry of the 4 rows of waveguides (old grill). The spectrum was calculated as a Fourier representation of the main waveguide mode electric field intensity along 50 magnetic lines equally spaced. The poloidal dependence of the electric field was taken into account. According to these computations, the effect of the peak width variation between possible q values (3 to 9) should be 20-25 %, what is in a reasonable agreement with Fig.10. The electron acceleration significantly decreases with increasing the tilt, when computed for a field of a single waveguide row [4], as the length of the electron trajectory is shorter in front of the waveguide row. However, when we computed the electron acceleration for an electron trajectory in the real geometry of the 4 rows of waveguides, the dependence of the mean electron acceleration on the tilt is not

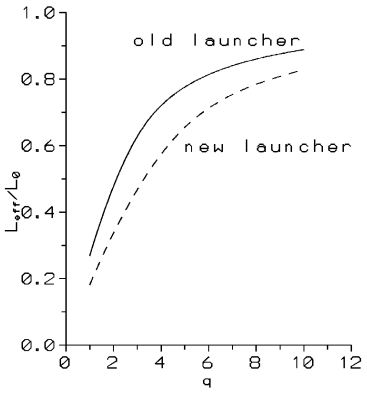

Fig. 10. Dependence of the normalized averaged length L_{eff}/L_0 on q.

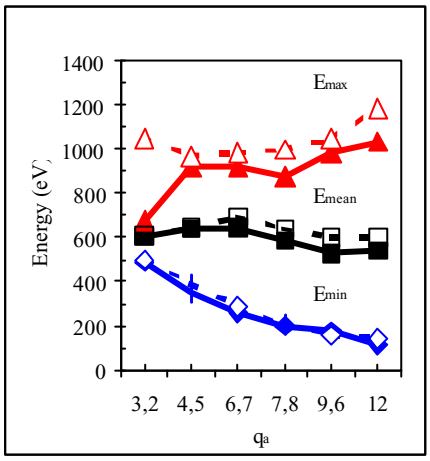

Fig.11. Computed mean (squares), minimum (diamonds), maximum (triangles) energy of 1000 electrons launched after travelling in front of an array of 4 rows of 32 waveguides in the ion-drift side (solid line, closed symbols) and electron-drift side (broken line, open symbols) vs the safety factor q_a.

strong, cf. Fig.11. This is because the electron trajectory continues in front of more than one waveguide rows. The electric field in each waveguide has a random value (<E> = 4.5kV/cm, δ(E)=1.4kV/cm). The initial velocity distribution of the launched electrons is Gaussian (E_0=20eV).We conclude that the vortex intensity does not significantly vary with the B-tilt.

Conclusion

Rather significant plasma density perturbations, electrostatic charge separation fields and plasma flows (plasma vortex) can develop in front of the grill mouth as a consequence of the electron acceleration. Variations of the vortex intensity with the B-tilt are not strong.

The support of grants GACR 202/00/1217 and GAAS A1043101 is acknowledged.

References:

[1] V. Fuchs et al., Phys. Plasmas 3 (1996) 4023; M. Goniche et al., Nuclear Fusion 38 (1998) 919; K.M. Rantamaki et al., Phys. Plasmas 5 (1998) 2553.
[2] V. Petrzilka et al., Proc. 28th EPS Conference, Madeira, 18-22 June 2001, p. 289 (CD).
[3] V. Petrzilka et al., 18th IAEA Conference, Sorrento 2000, paper CN-77/EXP4/07.
[4] V. Petrzilka et al., 2nd EPS Conference on RF Heating, Brussels, 1998, p.149.